The first series of alkali dipyrrinato complexes

Adeeb Al-Sheikh Ali, Judy Cipot-Wechsler, Sarah M. Crawford, Omar Selim, Rhonda L. Stoddard, T. Stanley Cameron, and Alison Thompson

Abstract: The first series of alkali dipyrrinato complexes is reported, encompassing lithium, sodium, and potassium salts of *meso*-unsubstituted and *meso*-aryl-substituted derivatives. By varying the substituents at the *meso* position, the intermolecular distance between the two nitrogen atoms and thus the κ^2-*N*,*N*-bidentate bite angle was altered, as confirmed by comparison of crystallographic structures of dipyrrin free-bases in the solid-state. The mode of bonding varies as the ionic radius of the metal ion increases: solid-state structures reveal lithium to be accommodated in the plane of the dipyrrinato unit, whilst sodium is accommodated out of plane. The reactivity of analogous lithium, sodium, and potassium dipyrrinato complexes increases as the ionic radius of the metal ion increases, in keeping with the concept that the complexes tend towards an increasingly ionic nature as the size of the alkali metal increases.

Key words: dipyrrin, dipyrrinato, alkali salts, monoanionic bidentate, *N*,*N*-chelation, pyrrolic.

Résumé : On rapporte la préparation de la première série de complexes dipyrrinato alcalins comportant les sels de lithium, de sodium et de potassium de dérivés *méso* non substitués et *méso* substitués par des groupes aryles. En faisant varier la nature des substituants en position méso, on modifie la distance intermoléculaire entre les deux atomes d'azote et, en conséquence, l'angle de morsure κ^2-*N*,*N* du bidentate, tel que confirmé par une comparaison des structures cristallographiques des bases libres dipyrrines à l'état solide. Le mode de liaison varie avec une augmentation du rayon ionique de l'ion métallique; les structures à l'état solide révèlent que le lithium s'accommode dans le plan de l'unité dipyrrinato alors que le sodium est accommodé hors du plan. La réactivité des complexes analogues du lithium, du sodium et du potassium augmente avec une augmentation du rayon ionique du métal ionique, en accord avec le concept que les complexes tendent vers une nature de plus en plus ionique avec une augmentation de la taille des métaux alcalins.

Mots-clés : dipyrrine, dipyrrinato, sels alcalins, bidentate monoanionique, *N*,*N*-chélation, pyrrolique.

[Traduit par la Rédaction]

Introduction

The N–*H* hydrogen atom of dipyrrins (Fig. 1), best-known for their presence in 4,4-difluoro-4-bora-3a,4a-diaza-*s*-indacenes (BODIPYs),[1] can be formally deprotonated to give the monoionic conjugated dipyrrinato species that can act as a bidentate ligand for the synthesis of supramolecular assemblies and discrete complexes.[2] Crucially, dipyrrinato ligands generally adopt a (*Z*)-*syn*-type arrangement and thus chelate in a κ^2 manner.[3,4] Although dipyrrinato metal complexes have been reported for M^+ species, such as thallium(I)[5] and rhodium(I),[6] alkali complexes involving the dipyrrinato ligand were unknown before our recent communication involving lithium.[7] We showed that the monoanionic source of the ligand, rather than the corresponding free base or its protonated derivative, gave access to unprecedented reactivity and previously inaccessible heteroleptic zinc(II) complexes. Our work was followed by an example whereby a lithium dipyrrinato complex was used to generate heteroleptic iron(II) and zinc(II) complexes.[8] Porphyrins, which can be formed from the condensation of two appropriately substituted dipyrrins, undergo deprotonation to give the di-ionic tetradentate ligand, and alkali metalloporphyrins have been well-documented,[9] as has the synthetic utility of such complexes in transmetallation reactions to obtain Ag(I), Zn(II), Cd(II), Hg(II), Cu(II), Sn(II), and Fe(III) complexes of porphyrins.[10] As lithium, sodium, and potassium complexes of porphyrins have all been reported,[11] we found it surprising that alkali complexes of the dipyrrinato ligand were unknown before our work, apart from a single example of a lithium-cryptand-dipyrrinato complex in solution:[12] such derivatives of related β-diketiminato (NacNac),[13,14] porphodimethene,[15] pyrroloimine,[16,17] and amino-pyrrole[18,19] skeletons are well-known.

Many recent advances in coordination chemistry and catalysis have been dependent upon the utility of stable *N*,*N*-bidentate monoanionic ligands. To this end, β-diketiminato ligands have attracted much attention as spectator ligands: they are isoelectronic to the cyclopentadienyl anion; they

Received 25 September 2009. Accepted 23 November 2009. Published on the NRC Research Press Web site at canjchem.nrc.ca on 26 April 2010.

This article is part of a Special Issue dedicated to Professor R. J. Boyd.

A.A. Ali,[1] J. Cipot-Wechsler, S.M. Crawford, O. Selim, R.L. Stoddard, T.S. Cameron, and A. Thompson.[2] Department of Chemistry, Dalhousie University, Halifax, NS B3H 4J3, Canada.

[1]Present address: Chemistry Department, Taibah University, Almadinah Almunawarah, P.O. Box: 30002, Saudi Arabia.
[2]Corresponding author (e-mail: Alison.Thompson@dal.ca).

Scheme 1. Synthesis of dipyrrins **1**–**3**.

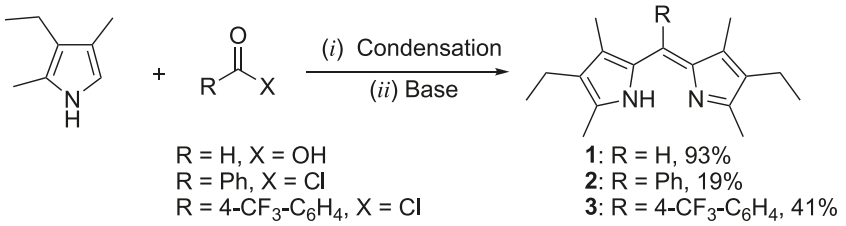

Fig. 1. Dipyrrin and the monoanionic dipyrrinato skeleton.

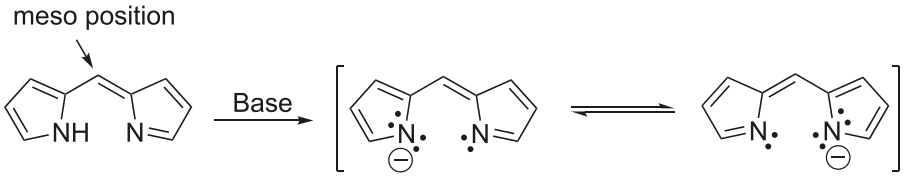

Fig. 2. Dipyrrinato skeleton as compared to the β-diketimato framework.

strongly coordinate to metal centers; and the reactivities of metal centers can be tuned by changing the steric and electronic properties of the substituents at the nitrogen atoms. The β-diketiminato ligand[20,21] has a similar *N*,*N*-bidentate monoionic framework to the dipyrrinato ligand (Fig. 2). However, the ability of the dipyrrinato unit to support catalytically active metal centers has yet to be systematically examined.[2] There are limited examples of dipyrrins used as chelating ligands for transition-metal fragments, with no examples to date exploring the potential catalytic utility of the resulting complexes, although, in a recent report, an iron(II) dipyrrinato complex was shown to undergo C–H bond amination from an organic azide, hinting towards functional possibilities.[8] The lack of systematic exploration is somewhat surprising given the likely useful structural features of the monoanionic dipyrrinato ligand, e.g., a hard nitrogen donor pair, the formation of a six-membered ring upon metal coordination, and access to derivatives bearing variable steric and electronic substituents. Traditionally, dipyrrinato complexes have been prepared using either HX salts or free-bases as the source of the ligand. Clearly, these ionization states limit the potential for the synthesis of dipyrrinato complexes with a diverse array of metal fragments, and it thus follows that alkali dipyrrinato complexes would be of interest.

One of the structural locations upon dipyrrinato ligands that can easily be modified is the *meso* position (Fig. 1). The term "*meso*" is borrowed from the chemistry of porphyrins, and is routinely applied to dipyrrins to identify the methylene position between the two pyrrolic units. By varying the substituents at the *meso* position, we hoped to alter the intermolecular distance between the two nitrogen atoms, and thus influence the C4–C5–C6 angle, and thus the bite angle, of the dipyrrinato ligand. As a result, the mode of bonding and the reactivity of the alkali dipyrrinato complexes would be anticipated to vary. Herein, we compare the solid-state structures of dipyrrinato salts and free-bases, and report our work regarding *meso*-unsubstituted and *meso*-substituted lithium, sodium, and potassium complexes involving the dipyrrinato ligand.

Results and discussion

To investigate the stability and properties of alkali dipyrrinato complexes, three free-base dipyrrins were synthesized (Scheme 1); one dipyrrin unsubstituted at the *meso* position and two new dipyrrins bearing aryl groups at the *meso* position. We maintained the symmetrical bis(1,3-dimethyl-2-ethyl) substitution pattern across the series by using kryptopyrrole in all of our syntheses. The *meso*-unsubstituted dipyrrin **1HBr**[22,23] was prepared by reacting kryptopyrrole with formic acid in the presence of HBr, and we then grew crystals of this salt via slow cooling of the reaction mixture. Liberation of the free-base **1** could be achieved using either lithium hydride or ammonium hydroxide.[7] The *meso*-phenyl and *meso*-*p*-CF_3-phenyl dipyrrins **2** and **3**, respectively, were prepared initially as their hydrochloride salts by reacting the corresponding acid chloride with kryptopyrrole. The salts were purified over silica gel to remove any unreacted starting materials as well as the major ketone byproduct (the structure of 4-ethyl-3,5-dimethyl-2-phenylacetylpyrrole, the intermediate en route to **2**, was confirmed using X-ray crystallography, see Experimental section). Treatment of **2HCl** and **3HCl** with satd. $NaHCO_3$ gave the requisite free-bases in analytically pure form after purification over basic alumina. The low yields of **2** and **3** were attributed to the steric and electronic factors of the persistent ketone intermediates.

Reacting a THF solution of free-base **1** with *n*BuLi gave clean conversion to the lithium dipyrrinato complex **4a** (Table 1), which was crystallographically characterized as **4a** and **4a**·$(THF)_2$.[7] As detailed in our previous communication, the structural features of **4a**·$(THF)_2$ are consistent with the relevant N–Li and N–C bond lengths of related lithium diketiminato complexes (β-diketiminato backbone substituted with either methyl[24] or *tert*-butyl groups[25]) that include at least one solvent ether molecule. However, the N–Li–O angles in **4a**·$(THF)_2$ are contracted relative to those of related lithium β-diketiminato structures containing only one

Table 1. Synthesis of *meso*-substituted alkali metal dipyrrinato complexes.

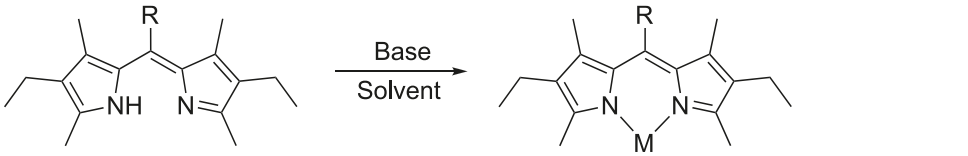

1: R = H
2: R = Ph
3: R = 4-CF_3-C_6H_4

R = H: **4a**, M = Li; **4b**, M = Na; **4c**, M = K
R = Ph: **5a**, M = Li; **5b**, M = Na; **5c**, M = K
R = 4-CF_3-C_6H_4: **6a**, M = Li; **6b**, M = Na; **6c**, M = K

Compound	R	Base	M	Solvent	Isolated yield (%)
4a	H	BuLi	Li	THF	95
4b	H	$NaN(SiMe_3)_2$	Na	Et_2O	74
4c	H	KCH_2Ph	K	THF	66
5a	Ph	BuLi	Li	THF	50
5b	Ph	$NaN(SiMe_3)_2$	Na	Et_2O	63
5c	Ph	$KN(SiMe_3)_2$	K	THF	73
6a	*p*-CF_3–Ph	$LiN(SiMe_3)_2$	Li	THF	81
6b	*p*-CF_3–Ph	$NaN(SiMe_3)_2$	Na	THF	91
6c	*p*-CF_3–Ph	$KN(SiMe_3)_2$	K	THF	83

coordinated solvent molecule (average 130.8°),[24,25] presumably due to steric crowding.

The THF-free solid-state structure of **4a** and the THF-supported structure exhibit significant differences in bond lengths and angles, as we previously reported.[7] For example, the N–Li average distance is 1.39(1) Å in **4a**, compared with 1.98(1) Å in **4a**·$(THF)_2$, akin to the Li–N bond length in related lithium diketiminato[13,14,25,26] and porphyrin complexes.[11] Furthermore, the acute C4–N1–Li and C6–N2–Li bond angles in **4a** are only 95.3(4)° and 96.4(4)°, respectively. The bond angles, the planarity of the six-membered chelate ring, and the short N–Li distances in the solid-state structure of **4a** are consistent with an otherwise uncoordinated lithium atom, which is somewhat of a rarity.[24]

The *meso*-unsubstituted sodium dipyrrinato complex (**4b**) was prepared via the slow addition of an ethereal solution of sodium bis(trimethylsilyl)amide to an ethereal solution of the free-base **1**. An orange precipitate was immediately formed, the reaction mixture was filtered over Celite, and the residue was washed with ether to remove unreacted free-base and other byproducts. Subsequently, the product was dissolved in THF, the solution was filtered over Celite, and then the solvent was removed in vacuo.

The *meso*-unsubstituted dipyrrinato sodium complex (**4b**) was crystallographically characterized after a suitable dark-red crystal was obtained from the slow evaporation of solvent from a concentrated THF solution. The X-ray structure of **4b** (Fig. 3) reveals an oligomer where complexed sodium ions are positioned within non-planar six-membered rings via *N*,*N*′-chelation, in contrast to the corresponding dipyrrinato lithium complex[7] whereby the lithium atom was found to be positioned between the two nitrogen atoms in a discrete planar six-membered ring. The structure of **4b** contains three unique sodium atoms: Na(1), which is on an inversion centre, Na(2), which is in a general position, and Na(3), which is on a twofold axis. Thus, while there are three unique sodium atoms, Na(1) and Na(3) have only half occupancy. The Na(1)–Na(2) distance is 3.247(1) Å, and the Na(2)–Na(3) distance is 3.541(2) Å. Although these are

Fig. 3. The X-ray structure of sodium dipyrrinato complex **4b**, shown with probability ellipsoids of 50% (hydrogen atoms and THF molecules omitted for clarity; the end of the oligomer and the attached side chains are disordered in two slightly different orientations; disorder not shown).

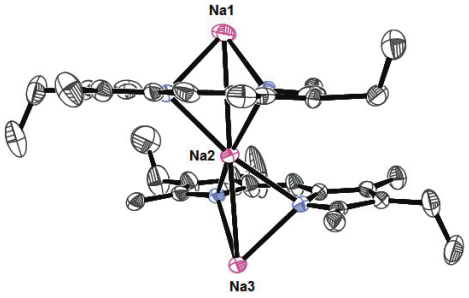

long, they are arguably just within a van der Waals radius, with the chain of sodium atoms of course propagated by the inversion centre giving a second Na(1)–Na(2) distance of 3.247(1) Å and a Na(3)–Na(2) distance of 3.541(2) Å. The coordination about Na(1) is a near-regular octahedron with two dipyrrinato units and two THF molecules, obviously with pairs related by the inversion centre. The coordination about Na(3) is an approximate five-coordinate square-based pyramidal system with two dipyrrinato units in the base and a THF molecule with its oxygen atom displaced just slightly off the twofold axis. The coordination about the central Na(2) atom is again five-coordinate with a very distorted square-based pyramid. The two dipyrrinato units are in the base but the THF molecule and its oxygen atom are well-displaced to one side. All of the ligands (except the THF molecule coordinated to Na(3)) do double duty, coordinating and bridging between two sodium atoms. Thus, between Na(1) and Na(2) there are two dipyrrinato units and the one (displaced) THF bridging the short (3.247 Å) Na(1)–Na(2) distance. However, a THF molecule is absent from the bridging position between Na(2) and Na(3), and just two dipyrrinato units bridge that longer gap (3.541(2) Å). In all,

the close approach of the sodium atoms to each other is a consequence of the bridging ligands and probably has no bonding significance.

The bond angles C4–C5–C6 and C21–C22–C23 for the two dipyrrinato units in the solid-state structure of **4b** were decreased to 132.9(3)° and 132.8(4)°, respectively, compared with 148.7(3)° in the free-base **1**. Although the C4–C5–C6 angles in **4b** were found to be close to those for the lithium dipyrrinato complex (**4a**), the larger ionic size of the sodium ion, compared with the lithium ion, prevented a planar geometry of the complex; as a result, the sodium ion is accommodated out of the dipyrrinato plane. As expected, the N–Na bond lengths of **4b** (average 2.53(4) Å) are longer than the N–Li bond lengths of **4a**·$(THF)_2$ (1.98(1) Å). Such a comparison suggests that the ionic nature of alkali dipyrrinato complexes increases as the ionic radii of the metal increase. Related sodium diketiminato complexes exhibit the same trend as our dipyrrin analogues, e.g., Na–N bond length of 2.395(6) Å (cf. Li–N bond length of 1.9975(7) Å[26]) with the lithium ion being accommodated in plane and the sodium ion being accommodated out of plane.

The *meso*-unsubstituted potassium dipyrrinato complex (**4c**) was prepared using benzyl potassium (KCH_2Ph) as the base. As KCH_2Ph[27] is insoluble in diethyl ether, THF was used as the reaction solvent. Upon the addition of a THF solution of benzyl potassium to a THF solution of the free-base **1**, the potassium dipyrrinato complex (**4c**) instantly precipitated as an orange solid. The solvent was removed in vacuo and the solid was washed with ether and then hexanes. The poor solubility of **4c** hindered attempts to secure a crystal suitable for crystallographic analysis, and despite much effort, we were unsuccessful in this regard. Furthermore, we were unable to crystallize any compounds bearing *meso*-aryl substituents.

Interested in how the C4–C5–C6 bond angle and the N–N intramolecular distance affect the coordination geometry of dipyrrinato complexes, we grew crystals of the three free-bases **1**–**3** via the slow evaporation of solvent from concentrated pentane solutions. With our hypothesis being that the nature of the *meso*-substituent would dramatically affect the C4–C5–C6 bond angle, and thus the N–N intramolecular distance and chelating bite angle, we were pleased that the X-ray crystallographic analysis revealed a dramatic decrease of the C4–C5–C6 angle from the *meso*-unsubstituted dipyrrin (**1**) [C4–C5–C6 bond angle, 148.7(3)°] (Fig. 4) to the substituted dipyrrins **2** [C4–C5–C6 bond angle, 124.8(2)°] (Fig. 5) and **3** [C4–C5–C6 bond angle, 124.1(2)°], respectively (Fig. 6). Moreover, as the C4–C5–C6 angle decreases across the series **1**–**3**, the intermolecular distance between the nitrogen atoms also decreases (2.73 Å for **1**, 2.69 Å for **2**, and 2.66 Å for **3**) and hence the bonding mode of complexation of the corresponding dipyrrinato ligands would be expected to vary, in terms of bite angle and so forth.

Despite the plethora of known dipyrrin salts and free-bases,[2] only a small number of refined crystal structures have been reported: the N–N intramolecular distances, the C4–C5–C6 angles, and the geometry across the central alkenyl bond of reported salts and free-bases are collated in Table 2, along with those for **1HBr**. Interestingly, the 148.7° C4–C5–C6 angle in the free-base **1** is much larger than in the known free-bases **7**[28] and **8**[29] (127.0° and 126.1°, respectively) and the salts **1HBr** (133.8°), **14**,[30] **15**,[31] **16**,[32] **17**,[33] and **18**[34] (within the range 132.1°–136.0°), despite the fact that all bear hydrogen atoms at the *meso* position. The significantly different sizes in the C4–C5–C6 angle are presumably a consequence of (*i*) the substituents that

Fig. 4. The X-ray structure of dipyrrin **1**, shown with probability ellipsoids of 50% (hydrogen atoms were omitted for clarity; the structure solves in either *Pbca* or in *Pca*21; *R* value in *Pbca* is 5.7%, and 5.1% in *Pca*21; the higher symmetry space group has been chosen; the pyrrole C and N atoms are in slightly disordered positions and the N–H hydrogen atom has not been located, since it sits on the disordered N–C bridge).

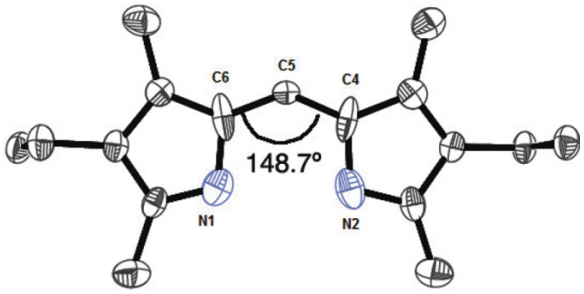

Fig. 5. The X-ray structure of dipyrrin **2**, shown with probability ellipsoids of 50% (hydrogen atoms were omitted for clarity).

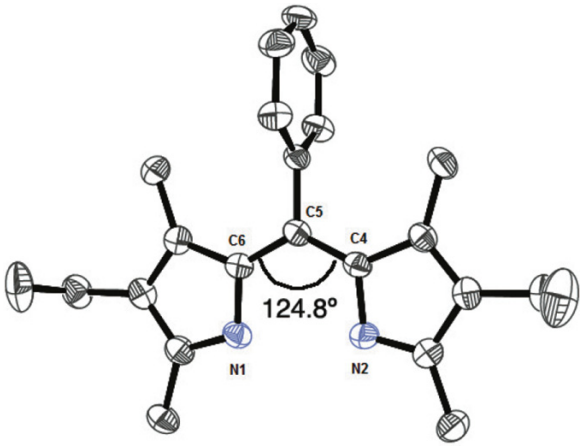

Fig. 6. The X-ray structure of dipyrrin **3**, shown with probability ellipsoids of 50% (hydrogen atoms were omitted for clarity; CH_2CH_3 disorder is not shown).

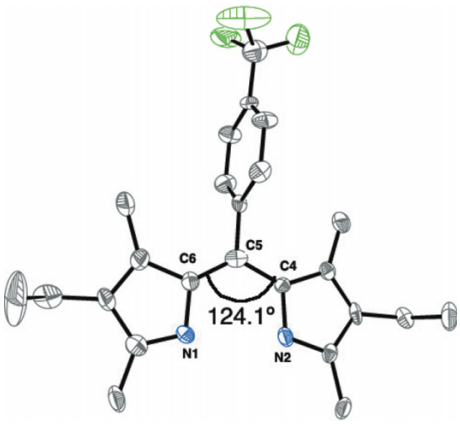

Table 2. N—N distance, C4–C5–C6 angle, and configuration for solid-state dipyrrins (geometric data rounded to ±0.01 Å and ±1°).

Structure	N—N distance (Å)	C4–C5–C6 angle (°)	Configuration
1HBr	3.27	134	*Z*
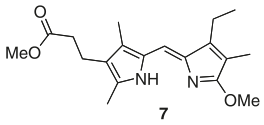 **7**	2.72	127	*Z*
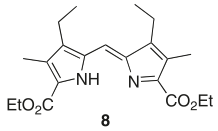 **8**	2.75	126	*Z*
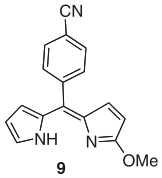 **9**	2.74	123	*Z*
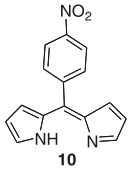 **10**	2.74	124	*Z*
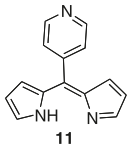 **11**	2.76	125	*Z*
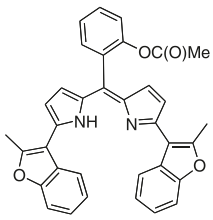 **12**	2.70	123	*Z*
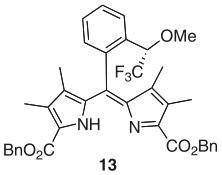 **13**	2.64	122	*Z*
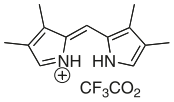 **14**	3.31	136	*Z*

Table 2 (*Concluded*).

Structure	N—N distance (Å)	C4–C5–C6 angle (°)	Configuration
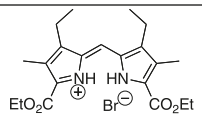 **15**	3.38	133	*Z*
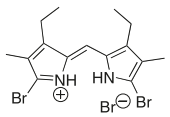 **16**	3.25	134	*Z*
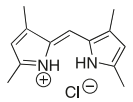 **17**	3.22	133	*Z*
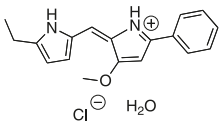 **18**	4.78	132	*E*
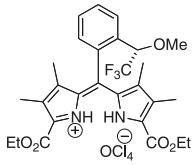 **19**	2.82	122	*Z*
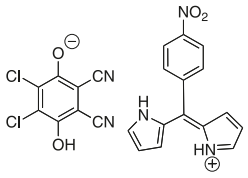 **20**	4.40	124	*Z*
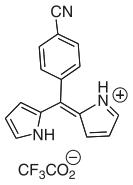 **21**	4.38	125	*E*
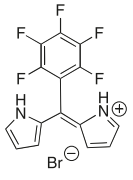 **22**	4.90	123	*E*

Scheme 2. Reactions of alkali dipyrrin complexes.

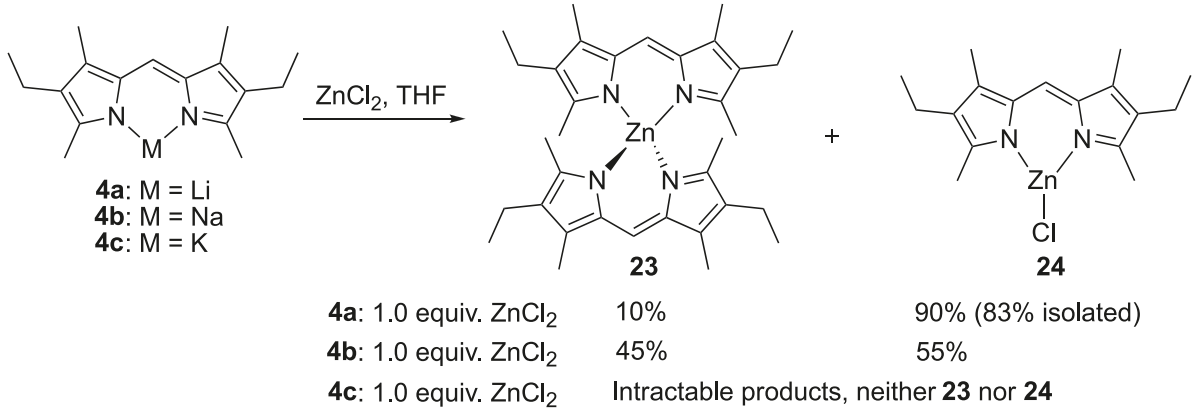

flank the *meso* position, and (*ii*) the strength and nature of the intramolecular NH–H hydrogen bonding in which the N-*H* hydrogen atom(s) partake(s).

Our *meso*-aryl free-bases **2** and **3** compare well with the known *meso*-aryl dipyrrin free-bases **9**,[35] **10**,[4] **11**,[36] **12**,[37] and **13**,[38] and the known dipyrrin salt **19**:[38] all exhibit *Z* configuration across the alkenyl bond, all have their N atoms aligned with syn geometry (as necessary for chelated complexation), all possess an N–N intramolecular distance of around 2.7 Å (2.8 Å for the salt), and all exhibit a C4–C5–C6 angle of 123°–124° (121.7° for the salt). As shown in Table 2, the *meso*-aryl substituted dipyrrin salts **20**,[4] **21**,[39] and **22**[40] exhibit either an *E* configuration or anti geometry, and therefore the C4–C5–C6 angles and N–N intramolecular distances cannot be usefully compared to those of **2** and **3**. All of the free-bases, whether *meso*-substituted or not, exhibit *Z* configuration across the central alkenyl bond, presumably to accommodate intramolecular NH–H hydrogen bonding. This configuration clearly predisposes the ability of such ligands to act as bidentate chelating ligands.

We previously reported[7] that the reaction of lithium dipyrrinato complex (**4a**) with $ZnCl_2$ gives unprecedented access to heteroleptic zinc complexes (Scheme 2). To further benchmark the reactivity of alkali dipyrrinato complexes as reagents in simple salt-elimination reactions, a solution of the sodium dipyrrinato complex (**4b**) in THF was added dropwise to a stirring solution of a stoichiometric amount of anhydrous $ZnCl_2$ in THF. After stirring for 1 h at room temperature, the solvent was removed in vacuo and a ^{1}H NMR spectrum of the crude material revealed a mixture of the homoleptic species **23**[23] and the heteroleptic species **24**[7] in approximately equal ratios (Scheme 2). Interestingly, although **23** and **24** are the only two products observed in the reaction of the dipyrrinato analogue **4a** with $ZnCl_2$, in that instance, the formation of the heteroleptic species **24** was by far dominant.[7] Thus, moving from the lithium salt to the sodium salt dramatically altered the course of the reaction. A similar reaction employing the potassium dipyrrinato analogue (**4c**) was also conducted, whereby a suspension of **4c** in THF was utilized, multiple and intractable products were thus generated, none of which were the known complexes **23** and **24**. This series of experiments reveals the differing reactivity of alkali dipyrrinato complexes and lends further support to the notion that the ionic nature of the complexes increases as the ionic radii of the metal increase.

With alkali dipyrrinato complexes of lithium, sodium, and potassium in hand, we turned our attention to the *meso*-aryl dipyrrins **2** and **3** to expand the series. Lithium (**5a**), sodium (**5b**), and potassium (**5c**) *meso*-phenyl dipyrrinato complexes were prepared using butyl lithium, sodium bis(trimethylsilyl)amide, and potassium bis(trimethylsilyl)amide, respectively, as the source of the metal ions. Similarly, the alkali *meso*-*p*-CF_3-C_6H_4 dipyrrinato complexes **6a**–**6c** were prepared from the corresponding free-base **3** using the metal bis(trimethylsilyl)amide as the source of the metal ion. The yields and procedures are summarized in Table 1. Taking advantage of the phenomenon that the dipyrrins **2** and **3** are soluble in pentane while the alkali complexes are not, the resultant *meso*-substituted alkali dipyrrinato metal complexes **5a**–**5c** and **6a**–**6c** were repeatedly washed with pentane to remove unreacted free-base and other byproducts. Unfortunately, and despite much effort, we were unsuccessful in growing X-ray-quality crystals of any alkali dipyrrinato complexes bearing *meso*-aryl substituents.

The ^{15}N NMR chemical shifts for dipyrrins, their salts, and their complexes are diagnostic,[23] and this technique generally allows for the characterization of nitrogen-containing heterocyclic compounds, as noted by others.[41–43] With our current work, the published ^{15}N dipyrrinato chemical-shift ranges[23] can now be expanded to include alkali dipyrrinato complexes. As indicated in Fig. 7, the ^{15}N chemical shifts for the complexes **4**–**6** reported here do not overlap with their corresponding free-base dipyrrins **1**–**3**. Indeed, the chemical shifts dramatically increase from the range of –162 to –164 ppm for the free-bases **1**–**3** to the range of –219 to –231 ppm for the alkali metal complexes **4**–**6**.

Curiously, the ^{13}C NMR spectra for the sodium and potassium dipyrrinato complexes with *meso*-aryl substituents exhibited low signal/noise ratios. Indeed, many more than the expected number of scans were required to attain signals for all of the carbon atoms, and with our expectations based on concentrations of solutions and our experience with other dipyrrinato complexes, we were unable to find a convincing rationale for this phenomenon but were nevertheless able to assign all signals.

Conclusions

In summary, this work represents the first synthesis and characterization of a series of alkali dipyrrinato complexes.

Fig. 7. ^{15}N chemical shifts, relative to nitromethane at 125.41 ppm.

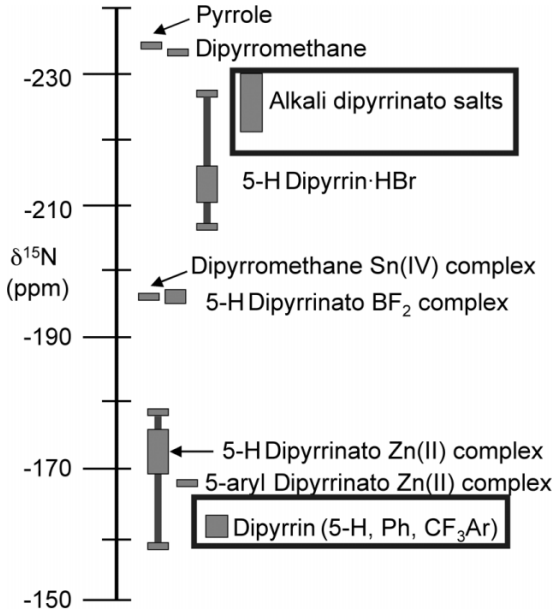

Three ligands bearing different substituents at the *meso* position have been utilized, along with lithium, sodium, and potassium metal ions. Variation of the substituent at the *meso* position altered the C4–C5–C6 angle of the dipyrrinato unit. The alkali dipyrrinato complexes were characterized on the basis of spectroscopic techniques, including ^{15}N NMR spectroscopy, which was used as a diagnostic indication for these compounds. In contrast to the lithium dipyrrinato complex (**4a**), which adopted κ^2-*N*,*N*-bidentate behaviour for the dipyrrinato ligand with the lithium ion nestled within the plane, the analogous sodium dipyrrinato complex (**4b**) showed a different mode of bonding whereby an oligomeric structure sets the sodium ions out of the κ^2-*N*,*N*-bidentate dipyrrinato plane. With increasing ionic radii of the alkali metals, relative reactivity increased when reactions with $ZnCl_2$ were investigated. Our current investigations include the use of alkali dipyrrinato complexes in salt elimination strategies to generate coordination complexes not previously accessible via the use of dipyrrin free-bases or their HX salts.

Experimental section

General procedures

Unless otherwise indicated, all manipulations were conducted in the absence of oxygen and water under an atmosphere of dinitrogen, either by using standard Schlenk methods, or within a glovebox apparatus, utilizing glassware that was oven-dried (130 °C) and evacuated while hot prior to use. Celite was oven-dried (130 °C) for 5 d and then evacuated for 24 h prior to use. The non-deuterated solvents: tetrahydrofuran, diethyl ether, toluene, benzene, hexanes, and pentane were deoxygenated and dried by sparging with dinitrogen gas, followed by passage through a double-column solvent-purification system. Tetrahydrofuran and diethyl ether were purified over two alumina-packed columns, while toluene, benzene, hexanes, and pentane were purified over one alumina-packed column and one column packed with copper-Q5 reactant. Sodium benzophenone ketyl was added to the solvent to provide visual confirmation (i.e., the observed persistence of the benzophenone ketyl) that an appropriate level of purification had been achieved. The solvents used within the glovebox were stored over activated 4 Å molecular sieves. THF-d_8 (Aldrich) and C_6D_6 (Aldrich) were degassed by using three repeated freeze–pump–thaw cycles and then dried over 4 Å molecular sieves for 24 h prior to use. HBr (48% aqueous solution), $LiN(SiMe)_2$, $NaN(SiMe)_2$, $KN(SiMe)_2$, *n*BuLi (1.6 mol/L solution in hexanes), silica gel (230–400 mesh, pH 6.5–7.5), and alumina (basic, grade 150, 58 Å) were all used as received. All nuclear magnetic resonance experiments were conducted using 250 and 500 MHz spectrometers. All chemical shifts (δ) are reported in ppm. All coupling constants (*J* =) are reported in Hz. All ^1H and ^{13}C NMR chemical shifts are reported relative to solvent peaks used as internal references: C_6D_6 (7.16 and 128.62 ppm, respectively), THF-d_8 (3.58 and 67.80 ppm, respectively), DMF-d_7 (8.03 and 163.15 ppm, respectively), and $CDCl_3$ (7.26 and 77.16 ppm, respectively). ^{15}N chemical shifts were obtained from two-dimensional ^1H (500 MHz) – ^{15}N (50.7 MHz) HMBC correlation experiments. ^{15}N, ^7Li, ^{23}Na, and ^{19}F shift scales were referenced as outlined in the IUPAC recommendations of 2001.[44] Mass spectra were obtained in ESI positive mode using a TOF instrument in both high and low resolution. All UV–vis analyses were performed using a 10 mm screw-cap cell (with Teflon tape), and solutions were prepared using glovebox techniques and dry THF. 4,4′-Diethyl-3,3′,5,5′-tetramethyldipyrrin hydrobromide (**1HBr**),[22] benzyl potassium,[27] 4,4′-diethyl-3,3′,5,5′-tetramethyldipyrrin (**1**),[7] and lithium 4,4′-diethyl-3,3′,5,5′-tetramethyldipyrrinato (**3a**)[7] were prepared according to literature procedures.

κ^2-(4,4′-Diethyl-3,3′,5,5′-tetramethyl-*meso*-C_6H_5-dipyrrin) (2)

To a solution of 3-ethyl-2,4-dimethylpyrrole (1.3 mL, 10 mmol) in $CHCl_3$ (50 mL), benzoyl chloride (70 mg, 5.0 mmol) was added, and the reaction mixture was heated at reflux temperature for 3 h. The resultant pink reaction mixture was extracted with water (2 × 30 mL), and the organic solution was then dried over Na_2SO_4. Removal of the organic solvent in vacuo gave crude material that was purified using chromatography on silica gel. A minor byproduct was eluted with 50% CH_2Cl_2 in hexane, and it was characterized to be 4-ethyl-3,5-dimethyl-2-phenyl acetylpyrrole as a pale yellow solid, mp 159–161 °C. δ_H (500 MHz, $CDCl_3$): 9.29 (1H, bs), 7.25–7.63 (5H, m), 2.38 (2H, q, *J* = 7.5), 2.35 (3H, s), 1.89 (3H, s), 1.05 (3H, t, *J* = 7.5). δ_C (125 MHz, $CDCl_3$): 185.7, 140.8, 133.1, 130.9, 128.9, 128.5, 128.4, 127.1, 125.5, 125.4, 123.9, 17.5, 15.3, 11.9, 11.7. δ_N (50.7 MHz, $CDCl_3$): –227.7. *m*/*z* (ESI$^+$): 250.1202 (M + Na)$^+$. A crystal of 4-ethyl-3,5-dimethyl-2-phenyl acetylpyrrole suitable for X-ray crystallographic analysis was grown via slow evaporation of a solution in hexane (structure included herein). The major band was eluted with 5% CH_3OH in CH_2Cl_2. Removal of the solvent in vacuo followed by dissolution in CH_2Cl_2 (30 mL) and then washing with saturated $NaHCO_3$ solution (2 × 30 mL) gave the title compound as its free-base. Drying of the solution over Na_2SO_4 and removal of the organic solvent in vacuo gave

an orange solid that was purified using column chromatography on basic alumina eluting with 60% CH_2Cl_2 in hexane to give the title compound as an orange solid (31 mg, 19%): mp 148–150 °C. UV–vis λ_{max} (nm): 515 (ϵ 45 000 mol/L^{-1}cm^{-1}, MeOH). δ_H (500 MHz, $CDCl_3$): 7.44–7.45 (3H, m), 7.34–7.36 (2H, m), 2.31 (6H, s), 2.28 (4H, q, J = 7.5), 1.19 (6H, s), 0.97 (6H, t, J = 7.5). δ_C (125 MHz, $CDCl_3$): 150.3, 139.2, 135.7, 134.9, 131.5, 129.8, 128.6, 128.2, 124.2, 17.8, 15.1, 14.6, 11.9. δ_N (50.7 MHz, THF-d_8): –162.1. m/z HR $(MH)^+$ $C_{23}H_{28}N_2$ calcd.: 332.2252, found: 333.2303. Anal. calcd. for $C_{23}H_{28}N_2$: C, 83.09; H, 8.49; N, 8.43. Found: C, 83.13; H, 8.54; N, 8.31.

κ²-(4,4′-Diethyl-3,3′,5,5′-tetramethyl-*meso*-*p*-CF_3-C_6H_4-dipyrrin) (3)

To a solution of 3-ethyl-2,4-dimethylpyrrole (0.34 mL, 2.50 mmol) in CH_2Cl_2 (30 mL), 4-trifluoromethylbenzoylchloride (260 mg, 1.25 mmol) was added, and the reaction mixture was heated at reflux temperature for 48 h. The resultant pink reaction mixture was extracted with water (2 × 30 mL), and the organic solution was then dried over Na_2SO_4. Removal of the organic solvent in vacuo gave a crude product that was purified using chromatography on silica gel. A minor byproduct was eluted with 50% CH_2Cl_2 in hexane, and it was characterized to be 4-ethyl-3,5-dimethyl-2-(trifluoromethylphenyl) acetylpyrrole as a pale yellow solid, mp 165–167 °C. UV–vis λ_{max} (nm): 523 (ϵ 40 000 mol/L^{-1}cm^{-1}, MeOH). δ_H (500 MHz, $CDCl_3$): 9.20 (1H, bs), 7.65–7.71 (4H, bs), 2.38 (2H, q, J = 7.5), 2.27 (3H, s), 1.85 (3H, s), 1.05 (3H, t, J = 7.5). δ_C (125 MHz, $CDCl_3$): 183.7, 143.9, 134.0, 132.4 (q, $J_{C–F}$ = 32.3), 128.9, 128.4, 126.7, 125.8, 125.4, 123.9 (q, $J_{C–F}$ = 270.8), 17.2, 15.1, 11.7, 11.6. δ_N (50.7 MHz, $CDCl_3$): –228.2. δ_F (243 MHz, $CDCl_3$): –63.7. m/z (ESI^-): 294.3 (M^-). The major band was eluted with 10% CH_3OH in CH_2Cl_2. Removal of the organic solvent in vacuo followed by dissolution of the solid in CH_2Cl_2 (30 mL) and then washing with satd. $NaHCO_3$ solution (2 × 30 mL) gave **3** as its free-base. Drying of the solution over Na_2SO_4 and removal of the organic solvent in vacuo gave an orange solid that was purified using column chromatography and basic alumina eluting with 50% CH_2Cl_2 in hexane to give the title compound as an orange solid (226 mg, 41%), mp (dec.) > 185 °C. δ_H (500 MHz, $CDCl_3$): 13.22 (1H, bs), 7.69 (2H, d, J = 10.0), 7.46 (2H, d, J = 10.0), 2.32 (6H, s), 2.27 (4H, q, J = 7.5), 1.15 (6H, s), 0.97 (6H, t, J = 7.5). δ_C (125 MHz, $CDCl_3$): 150.7, 142.8, 135.7, 135.4, 134.3, 131.8, 130.4 (q, $J_{C–F}$ = 32.3), 130.2, 125.4, 124.2 (q, $J_{C–F}$ = 265.0), 17.6, 14.8, 14.4, 12.0. δ_F (243 MHz, $CDCl_3$): –63.3. δ_N (50.7 MHz, $CDCl_3$): –163.6. m/z $(MH)^+$ HR $C_{24}H_{27}F_3N_2$ calcd.: 400.2126, found: 401.2187. Anal. calcd. for $C_{24}H_{27}F_3N_2$: C, 71.98; H, 6.80; N, 6.99. Found: C, 72.16; H, 6.82; N, 6.85.

κ²-(4,4′-Diethyl-3,3′,5,5′-tetramethyldipyrrinato) sodium (4b)

In a glovebox, an Et_2O (2 mL) solution of $NaN(SiMe_3)_2$ (40 mg, 0.22 mmol) was added dropwise over 5 min to a magnetically stirring solution of **1** (57 mg, 0.22 mmol) in Et_2O (2 mL). Upon addition of the base, a bright orange solid immediately precipitated from the reaction mixture. After 1 h, the reaction mixture was filtered over Celite and the residue was washed with ether (4 × 2 mL) to remove any impurities and the $HN(SiMe_3)_2$ byproduct. The product was dissolved in THF (2 mL) and filtered through Celite. Slow evaporation of the solvent from the filtrate resulted in the formation of large red plate crystals. These were isolated and dried in vacuo to leave the title compound as red crystals (46 mg, 74%). δ_H (500 MHz, THF-d_8): 6.75 (1H, s), 2.35 (4H, q, J = 7.5), 2.16 (6H, s), 2.11 (6H, s), 1.00 (6H, t, J = 7.5). δ_C (125 MHz, THF-d_8): 153.8, 138.2, 135.3, 128.2, 123.2, 19.4, 16.6, 16.2, 10.5. δ_N (50.7 MHz, THF-d_8): –225.4. δ_{Na} (132.3 MHz, THF-d_8): 10.7.

κ²-(4,4′-Diethyl-3,3′,5,5′-tetramethyldipyrrinato) potassium (4c)

In a glovebox, a THF (2 mL) solution of KCH_2Ph[27] (25 mg, 0.20 mmol) was added dropwise over 5 min to a solution of **1** (50 mg, 0.20 mmol) in THF (2 mL). Upon addition of the base, a bright orange solid precipitated from the reaction mixture. The reaction vial was sealed and the contents manually shaken for 30 s then left at room temperature. After 1 h, the solvent was removed in vacuo and the orange solid was washed with Et_2O (2 × 2 mL) and then hexanes (3 × 2 mL) to remove any impurities and byproducts. Contrary to the sodium complex, the potassium analogue was found to be insoluble in THF. Therefore, the supernatants were removed in each case by allowing the solid to settle and then carefully decanting the liquid away. The resulting orange solid was dried in vacuo to leave the title compound (37 mg, 66%). δ_H (500 MHz, DMF-d_7): 6.80 (1H, s), 2.34 (4H, q, J = 7.5), 2.18 (6H, s), 2.13 (6H, s), 1.00 (6H, t, J = 7.5). δ_C (125 MHz, DMF-d_7): 153.3, 137.9, 134.6, 132.0, 127.3, 19.3, 16.4, 15.9, 10.7. δ_N (50.7 MHz, DMF-d_7): –221.4.

κ²-(4,4′-Diethyl-3,3′,5,5′-tetramethyl-*meso*-C_6H_5-dipyrrinato) lithium (5a)

In a glovebox, *n*BuLi (94 μL of a 1.6 mol/L hexanes solution, 0.15 mmol) was added dropwise over 5 min to a solution of **2** (50 mg, 0.15 mmol) in THF (3 mL). Upon addition of the base, the colour of the solution immediately changed from orange to dark red-brown. The reaction vial was sealed and the contents were magnetically stirred for 45 min. The solvent was then removed in vacuo and the red-brown solid was washed with pentane (5 × 2 mL) to remove any impurities and byproducts. The supernatants were removed in each case by allowing the solid to settle and carefully decanting the liquid away. The resulting solid was dried in vacuo to give the title compound as a red solid (25 mg, 50%). δ_H (500 MHz, THF-d_8): 7.40–7.20 (5H, m), 2.25 (4H, q, J = 7.5), 2.20 (6H, s), 1.08 (6H, s), 0.92 (6H, t, J = 7.5). δ_C (125 MHz, THF-d_8): 153.3, 145.2, 138.6, 135.8, 131.9, 131.7, 130.7, 128.6, 127.8, 19.1, 16.0, 15.8, 13.3. δ_N (50.7 MHz, THF-d_8): –226.0. δ_{Li} (194.4 MHz, THF-d_8): 2.02.

κ²-(4,4′-Diethyl-3,3′,5,5′-tetramethyl-*meso*-C_6H_5-dipyrrinato) sodium (5b)

In a glovebox, a solution of $NaN(SiMe_3)_2$ (28 mg, 0.16 mmol) in Et_2O (2 mL) was added dropwise over 5 min to a magnetically stirring solution of **2** (51 mg, 0.16 mmol)

in Et_2O (2 mL). Upon addition of the base, the colour of the solution changed from orange to red. After 1 h, the solvent was removed in vacuo and the resulting solid was triturated/washed with pentane (5 × 2 mL) to remove any impurities and any byproducts. The supernatants were removed in each case by allowing the solid to settle and carefully decanting the liquid away. The resulting orange solid was dried in vacuo to give the title compound as a red solid (35 mg, 63%). δ_H (500 MHz, THF-d_8): 7.30–7.18 (5H, m), 2.27 (4H, q, J = 7.4), 2.16 (6H, s), 1.14 (6H, s), 0.94 (6H, t, J = 7.4). δ_C (125 MHz, THF-d_8): 153.3, 146.8, 144.3, 140.3, 134.8, 132.7, 131.0, 128.25, 128.0, 19.4, 16.3, 16.0, 13.3. δ_N (50.7 MHz, THF-d_8): –221.5. δ_{Na} (132.3 MHz, THF-d_8): 9.9.

κ²-(4,4′-Diethyl-3,3′,5,5′-tetramethyl-*meso*-C_6H_5-dipyrrinato) potassium (5c)

In a glovebox, a solution of $KN(SiMe_3)_2$ (30 mg, 0.15 mmol) in THF (2 mL) was added dropwise over 5 min to a magnetically stirring solution of **2** (50 mg, 0.15 mmol) in THF (2 mL). Upon addition of the base, the colour of the solution changed from orange to dark purple. After 1 h, the solvent was removed in vacuo and the resulting solid was triturated/washed with pentane (5 × 2 mL) to remove any impurities and any byproducts. The product was dissolved in THF (2 mL) and filtered through Celite. The resulting solid was dried in vacuo to give the title compound as a red solid (41 mg, 73%). δ_H (500 MHz, THF-d_8): 7.26–7.15 (5H, m), 2.31 (4H, q, J = 7.5), 2.07 (6H, s), 1.39 (6H, s), 0.98 (6H, t, J = 7.5). δ_C (125 MHz, THF-d_8): 153.5, 146.8, 145.3, 141.5, 133.9, 133.4, 131.9, 128.2, 128.2, 19.4, 16.1, 16.0, 13.2. δ_N (50.7 MHz, THF-d_8): –211.9.

κ²-(4,4′-Diethyl-3,3′,5,5′-tetramethyl-*meso*-*p*-CF_3-C_6H_4-dipyrrinato) lithium (6a)

In a glovebox, a solution of $LiN(SiMe_3)_2$ (41 mg, 0.25 mmol) in THF (4 mL) was added dropwise to a solution of **3** (100 mg, 0.25 mmol) in THF (2 mL). Upon addition of the base, the colour of the solution immediately changed from dark yellow-brown to dark red-brown. The reaction vial was sealed and the contents magnetically stirred for 2 h. The solvent was then removed in vacuo and the resulting red-brown solid was washed with hexane (5 × 2 mL) to remove any unreacted starting materials and byproducts. The residue was dissolved in THF and filtered over Celite. The solvent was removed in vacuo to give the title compound as a red solid (82 mg, 81%). δ_H (500 MHz, THF-d_8): 7.62 (2H, d, J = 8.0), 7.38 (2H, d, J = 8.0), 2.22 (4H, q, J = 7.5), 2.17 (6H, s), 1.03 (6H, s), 0.88 (6H, t, J = 7.5). δ_C (125 MHz, THF-d_8): 154.1, 149.3, 144.0, 138.2, 135.4, 132.5, 131.4, 130.2 (q, $J_{C–F}$ = 31.8), 125.9 (q, $J_{C–F}$ = 269.8), 125.6 (q, 2C, $J_{C–F}$ = 7.1), 19.1, 16.0, 15.5, 13.6. δ_F (243 MHz, THF): –61.6. δ_N (50.7 MHz, THF-d_8): –226.9. δ_{Li} (194.4 MHz, THF-d_8): 2.0.

κ²-(4,4′-Diethyl-3,3′,5,5′-tetramethyl-*meso*-*p*-CF_3-C_6H_4-dipyrrinato) sodium (6b)

In a glovebox, a solution of $NaN(SiMe_3)_2$ (46 mg, 0.25 mmol) in THF (4 mL) was added dropwise to a solution of **3** (100 mg, 0.25 mmol) in THF (2 mL). Upon addition of the base, the colour of the solution immediately changed from dark yellow-brown to dark purple. The reaction vial was sealed and the contents magnetically stirred for 2 h. The solvent was then removed in vacuo and the red-brown solid was washed with hexane (5 × 2 mL) to remove any unreacted starting materials and byproducts. The residue was dissolved in THF and filtered over Celite. The solvent was removed in vacuo to leave the title compound as a dark-red solid (96 mg, 91%). δ_H (500 MHz, THF-d_8): 7.55–7.62 (2H, m), 7.19–7.41 (2H, m), 2.27 (4H, q, J = 7.5), 2.18 (6H, s), 1.10 (6H, s), 0.94 (6H, t, J = 7.5). δ_C (125 MHz, THF-d_8): 153.7, 149.0, 144.6, 139.8, 135.7, 133.2, 131.8, 130.3 (q, $J_{C–F}$ = 30.6), 125.9 (q, $J_{C–F}$ = 270.1), 125.4, 19.2, 16.0, 15.9, 13.3. δ_F (243 MHz, THF): –60.1. δ_N (50.7 MHz, THF-d_8): –219.0. δ_{Na} (132.3 MHz, THF-d_8): 9.0.

κ²-(4,4′-Diethyl-3,3′,5,5′-tetramethyl-*meso*-*p*-CF_3-C_6H_4-dipyrrinato) potassium (6c)

In a glovebox, a solution of $KN(SiMe_3)_2$ (50 mg, 0.25 mmol) in THF (4 mL) was added dropwise to a solution of **3** (100 mg, 0.25 mmol) in THF (2 mL). Upon addition of the base, the colour of the solution immediately changed from dark yellow-brown to dark purple. The reaction vial was sealed and the contents magnetically stirred for 2 h. The solvent was then removed in vacuo and the red-brown solid was washed with hexane (5 × 2 mL) to remove any unreacted starting materials and byproducts. The residue was dissolved in THF and filtered over Celite. The solvent was removed in vacuo to give the title compound as a red solid (93 mg, 83%). δ_H (500 MHz, THF-d_8): 7.50 (2H, d, J = 7.8), 7.35 (2H, d, J = 7.8), 2.35 (4H, q, J = 7.5), 2.10 (6H, s), 1.41 (6H, s), 1.01 (6H, t, J = 7.5). δ_C (125 MHz, THF-d_8): 153.5, 148.7, 144.4, 141.0, 133.3, 133.1, 132.0, 129.9 (q, $J_{C–F}$ = 31.9), 125.7, 125.4 (q, $J_{C–F}$ = 270), 19.3, 16.0, 15.9, 13.2. δ_F (243 MHz, THF): –61.0 ppm. δ_N (50.7 MHz, THF-d_8): –226.0.

X-ray crystallographic data

Diffractometer: Rigaku RAXIS-UNKNOWN, Mo Kα radiation (λ = 0.71070 or 0.71075 Å). The structures were solved by direct methods[45] and expanded using Fourier techniques.[46] Some non-hydrogen atoms were refined anisotropically, while the rest were refined isotropically. Some hydrogen atoms were refined isotropically, the rest were included in fixed positions. The final cycle of full-matrix least-squares refinement (minimized to $\Sigma w(|F_o| - |F_c|)^2$ where w = least squares weights on F) was based on 3284 observed reflections ($I > 3.00\sigma(I)$) and 271 variable parameters and converged with unweighted and weighted agreement factors of $R = \Sigma||F_o| - |F_c||/\Sigma|F_o| = 0.0394$; $R_w = [\Sigma w(|F_o| - |F_c|)^2/\Sigma wF_o^2]^{1/2} = 0.0443$. The standard deviation of an observation of unit weight (standard deviation of an observation of unit weight $[\Sigma w(|F_o| - |F_c|)^2/(N_o - N_v)]^{1/2}$ where N_o = number of observations and N_v = number of variables) was 1.06. A Robust-resistant weighting scheme was used.[47] Plots of $\Sigma w(|F_o| - |F_c|)^2$ versus $|F_o|$, reflection order in data collection, sin θ/λ, and various classes of indices showed no unusual trends. The maximum and minimum peaks on the final difference Fourier map corresponded to 0.78 and –0.72 e/Å^3, respectively. Neutral atom scattering factors were taken from Cromer and Waber.[48] Anomalous dispersion effects were included in $F_{calcd.}$;[49] the values for $\Delta f'$ and $\Delta f''$ were those of Creagh and McAuley.[50] The

values for the mass attenuation coefficients are those of Creagh and Hubbell.[51] All calculations were performed using the CrystalStructure[52,53] crystallographic software package.

κ²-(4,4′-Diethyl-3,3′,5,5′-tetramethyldipyrrin) hydrobromide (1HBr)

$C_{17}H_{25}BrN_2$ (337.30), orange feathers, primitive monoclinic, space group $P2_1/a$ (No. 14), a = 8.7480(6) Å, b = 24.241(1) Å, c = 9.1766(6) Å, β = 118.248(2)°, V = 1714.2(2) Å^3, Z = 4, T = 24 °C, 2θ = 145.3°. Residuals: R ($I > 3.00\sigma(I)$) = 0.0492, residuals: R_w ($I > 3.00\sigma(I)$) = 0.0600, GoF = 1.063.

κ²-(4,4′-Diethyl-3,3′,5,5′-tetramethyldipyrrin) (1)

$C_{17}H_{24}N_2$ (256.39), orange needles, primitive orthorhombic, space group *Pbca* (No. 61), a = 12.8407(4) Å, b = 8.3486(3) Å, c = 13.9647(5) Å, V = 1497.04(9) Å^3, Z = 4, T = –150 °C, 2θ = 144.8°. Residuals: R ($I > 3.00\sigma(I)$) = 0.0577, residuals: R_w ($I > 3.00\sigma(I)$) = 0.0659, GoF = 1.139.

κ²-(4,4′-Diethyl-3,3′,5,5′-tetramethyl-*meso*-C_6H_5-dipyrrin) (2)

$C_{23}H_{28}N_2$ (332.49), yellow needle crystal, primitive monoclinic, space group $P2_1/n$ (No. 14), a = 11.1861(5) Å, b = 15.7267(7) Å, c = 11.1134(5) Å, β = 96.876(3)°, V = 1941.0(2) Å^3, Z = 4, T = –150 °C, 2θ = 61.3°. Residuals: R_w ($I > 3.00\sigma(I)$) = 0.0481, residuals: R_w ($I > 3.00\sigma(I)$) = 0.0537, GoF = 1.152.

κ²-(4,4′-Diethyl-3,3′,5,5′-tetramethyl-*meso*-p-CF_3-C_6H_4-dipyrrin) (3)

$C_{24}H_{27}N_2F_3$ (400.49), golden-orange, needle-plate, primitive orthorhombic, space group *Pbca* (No. 61), a = 19.230(1) Å, b = 9.6655(5) Å, c = 22.594(2) Å, V = 4199.4(5) Å^3, Z = 8, T = –173 °C, 2θ = 61.0°. Residuals: R ($I > 3.00\sigma(I)$) = 0.0394, residuals: R_w ($I > 3.00\sigma(I)$) = 0.0443, GoF = 1.057.

κ²-(4,4′-Diethyl-3,3′,5,5′-tetramethyldipyrrinato) sodium (4b)

$C_{40}H_{58}O_{1.5}Na_2$ (664.90), dark-red prism crystal, C-centered monoclinic, space group $C2/c$ (No. 15), a = 23.966(6) Å, b = 12.591(3) Å, c = 26.789(6) Å, β = 101.055(5)°, V = 7934(3) Å^3, Z = 8, T = –173 °C, 2θ = 68.1°. Residuals: R_w ($I > 3.00\sigma(I)$) = 0.0695, residuals: R_w ($I > 3.00\sigma(I)$) = 0.0794, GoF = 1.040.

4-Ethyl-3,5-dimethyl-2-phenylacetylpyrrole

$C_{15}H_{17}NO$ (227.31), dark-red crystal, C-centered monoclinic, space group $C2/c$ (No. 15), a = 27.818(1) Å, b = 7.3187(2) Å, c = 14.4726(8) Å, β = 119.151(2)°, V = 2573.3(2) Å^3, Z = 8, T = –150 °C, 2θ = 144.7°. Residuals: R_w ($I > 3.00\sigma(I)$) = 0.0392, residuals: R_w ($I > 3.00\sigma(I)$) = 0.0505, GoF = 1.033.

Supplementary data

Supplementary data for this article are available on the journal Web site (canjchem.nrc.ca). CCDCs 758519–758524 contain the X-ray data in CIF format for this manuscript. These data can be obtained, free of charge, via www.ccdc.cam.ac.uk/conts/retrieving.html (or from the Cambridge Crystallographic Data Centre, 12 Union Road, Cambridge CB2 1EZ, UK; fax +44 1223 336033; or deposit@ccdc.cam.ac.uk).

Acknowledgement

We thank the Natural Sciences and Engineering Research Council of Canada (NSERC) for financial support, and Dr. Laura Turculet (Dalhousie University) for providing benzyl potassium.

References

(1) Loudet, A.; Burgess, K. *Chem. Rev.* **2007**, *107* (11), 4891. doi:10.1021/cr078381n. PMID:17924696.
(2) Wood, T. E.; Thompson, A. *Chem. Rev.* **2007**, *107* (5), 1831. doi:10.1021/cr050052c. PMID:17430001.
(3) Falk, H. *The Chemistry of Linear Oligopyrroles and Bile Pigments*; Springer-Verlag: New York, 1989.
(4) Shin, J.-Y.; Dolphin, D. *CrystEngComm* **2008**, *10* (8), 960. doi:10.1039/b800367j.
(5) Hsieh, A. T. T.; Rogers, C. A.; West, B. O. *Aust. J. Chem.* **1976**, *29*, 49.
(6) Roomi, M. W. *Tetrahedron Lett.* **1974**, *15* (13), 1131. doi:10.1016/S0040-4039(01)82425-4.
(7) Cipot-Wechsler, J.; Ali, A. A.; Chapman, E. E.; Cameron, T. S.; Thompson, A. *Inorg. Chem.* **2007**, *46* (26), 10947. doi:10.1021/ic701369h. PMID:18027930.
(8) King, E. R.; Betley, T. A. *Inorg. Chem.* **2009**, *48* (6), 2361. doi:10.1021/ic900219b.
(9) Arnold, J. In *The Porphyrin Handbook* Kadish, K. M., Smith, K. M., Guilard, R., Eds.; Academic Press: 1999; Vol. 3.
(10) Dorough, G. D.; Miller, J. R.; Huennekens, F. M. *J. Am. Chem. Soc.* **1951**, *73* (9), 4315. doi:10.1021/ja01153a085.
(11) Arnold, J.; Dawson, D. Y.; Hoffman, C. G. *J. Am. Chem. Soc.* **1993**, *115* (7), 2707. doi:10.1021/ja00060a020.
(12) Seel, C.; Nieger, M.; Vogtle, F. *Chem. Ber.* **1992**, *125* (2), 447. doi:10.1002/cber.19921250223.
(13) Hitchcock, P. B.; Lappert, M. F.; Layh, M. *Dalton Trans.* **2001**, 2409.
(14) Stender, M.; Eichler, B. E.; Hardman, N. J.; Power, P. P.; Prust, J.; Noltemeyer, M.; Roesky, H. W. *Inorg. Chem.* **2001**, *40* (12), 2794. doi:10.1021/ic001311d. PMID:11375697.
(15) Benech, J.-M.; Bonomo, L.; Solari, E.; Scopelliti, R.; Floriani, C. *Angew. Chem. Int. Ed.* **1999**, *38* (13-14), 1957. doi:10.1002/(SICI)1521-3773(19990712)38:13/14<1957::AID-ANIE1957>3.0.CO;2-1.
(16) Liang, L.-C.; Yang, C.-W.; Chiang, M. Y.; Hung, C.-H.; Lee, P.-Y. *J. Organomet. Chem.* **2003**, *679* (1), 135. doi:10.1016/S0022-328X(03)00555-2.
(17) Love, J. B.; Blake, A. J.; Wilson, C.; Reid, S. D.; Novak, A.; Hitchcock, P. B. *Chem. Commun. (Camb.)* **2003**, (14): 1682. doi:10.1039/b303611a.
(18) Huang, J.-H.; Chi, L.-S.; Yu, R.-C.; Jiang, G. J.; Yang, W.-T.; Lee, G.-H.; Peng, S.-M. *Organometallics* **2001**, *20* (26), 5788. doi:10.1021/om010198b.
(19) Klappa, J. J.; Geers, S. A.; Schmidtke, S. J.; MacManus-Spencer, L. A.; McNeill, K. *Dalton Trans.* **2004**, (6): 883. doi:10.1039/b315523d. PMID:15252473.
(20) Bourget-Merle, L.; Lappert, M. F.; Severn, J. R. *Chem. Rev.* **2002**, *102* (9), 3031. doi:10.1021/cr010424r. PMID:12222981.

(21) Piers, W. E.; Emslie, D. J. H. *Coord. Chem. Rev.* **2002**, *233–234*, 131. doi:10.1016/S0010-8545(02)00016-4.
(22) Tu, B.; Wang, C.; Ma, J. *Org. Prep. Proced. Int.* **1999**, *31* (3), 349. doi:10.1080/00304949909458333.
(23) Wood, T. E.; Berno, B.; Beshara, C. S.; Thompson, A. *J. Org. Chem.* **2006**, *71* (8), 2964. doi:10.1021/jo0524932. PMID:16599589.
(24) Stender, M.; Wright, R. J.; Eichler, B. E.; Prust, J.; Olmstead, M. M.; Roesky, H. W.; Power, P. P. *J. Chem. Soc., Dalton Trans.* **2001**, (23): 3465. doi:10.1039/b103149j.
(25) Budzelaar, P. H. M.; Bart van Oort, A.; Orpen, A. G. *Eur. J. Inorg. Chem.* **1998**, 1485. doi:10.1002/(SICI)1099-0682(199810)1998:10<1485::AID-EJIC1485>3.0.CO;2-F.
(26) Farwell, J. D.; Hitchcock, P. B.; Lappert, M. F. *Chem. Commun. (Camb.)* **2002**, (5): 456. doi:10.1039/b110443h. PMID: 12120539.
(27) Schlosser, M.; Hartmann, J. *Angew. Chem.* **1973**, *12*, 508.
(28) Dattagupta, J. K.; Meyer, E. F. J.; Cullen, D. L.; Falk, H.; Gergely, S., Acta Crystallogr. *Sect. C: Cryst. Struct. Commun.* **1983**, *39*, 1384. doi:10.1107/S0108270183008604.
(29) Sheldrick, W. S.; Borkenstein, A.; Stuckmeier, G.; Engel, J. *Acta Crystallogr.* **1978**, *B34*, 329.
(30) Datta, S.; Lightner, D. A. *Monatsh. Chem.* **2008**, *139* (9), 1113. doi:10.1007/s00706-008-0888-2.
(31) Struckmeier, G.; Engel, J.; Thewalt, U., Z. Naturforsch. *B: Chem. Sci.* **1978**, *33*, 753.
(32) Becker, W.; Sheldrick, W. S.; Engel, J. *Acta Crystallogr.* **1978**, *B34*, 1021.
(33) Sessler, J. L.; Eller, L. R.; Cho, W.-S.; Nicolaou, S.; Aguilar, A. L., J.T.; Lynch, V. M.; Magda, D. J. *Angew. Chem. Int. Ed.* **2005**, *44*, 5989. doi:10.1002/anie.200501740.
(34) Melvin, M. S.; Tomlinson, J. T.; Park, G.; Day, C. S.; Saluta, G. R.; Kucera, G. L.; Manderville, R. A. *Chem. Res. Toxicol.* **2002**, *15* (5), 734. doi:10.1021/tx025507x. PMID: 12018996.
(35) Halper, S. R.; Stork, J. R.; Cohen, S. M. *Dalton Trans.* **2007**, (10): 1067. doi:10.1039/b615801c. PMID:17325783.
(36) Stork, J. R.; Thoi, V. S.; Cohen, S. M. *Inorg. Chem.* **2007**, *46* (26), 11213. doi:10.1021/ic7016159. PMID:18047326.
(37) Cavaleiro, J. A. S.; Condesso, F. P. N.; Olmstead, M. M.; Oram, D. E.; Snow, K. M.; Smith, K. M. *J. Org. Chem.* **1988**, *53* (25), 5847. doi:10.1021/jo00260a009.
(38) Gossauer, A.; Nydegger, F.; Kiss, T.; Sleziak, R.; Stoeckli-Evans, H. *J. Am. Chem. Soc.* **2004**, *126* (6), 1772. doi:10.1021/ja030542r. PMID:14871109.
(39) Salazar-Mendoza, D.; Baudron, S. A.; Hosseini, M. W. *Inorg. Chem.* **2008**, *47* (3), 766. doi:10.1021/ic701949k. PMID:18177038.
(40) Shin, J.-Y.; Dolphin, D.; Patrick, B. O. *Cryst. Growth Des.* **2004**, *4* (4), 659. doi:10.1021/cg049979g.
(41) Bonnier, C.; Piers, W. E.; Parvez, M.; Sorensen, T. S. *Chem. Commun. (Camb.)* **2008**, (38): 4593. doi:10.1039/b808739c. PMID:18815694.
(42) Dogutan, D. K.; Zaidi, S. H. H.; Thamyongkit, P.; Lindsey, J. S. *J. Org. Chem.* **2007**, *72* (20), 7701. doi:10.1021/jo701294d. PMID:17824652.
(43) Strong, E. T. J.; Cardile, S. A.; Brazeau, A. L.; Jennings, M. C.; McDonald, R.; Jones, N. D. *Inorg. Chem.* **2008**, *47* (22), 10575. doi:10.1021/ic8011926. PMID:18928277.
(44) Harris, R. K.; Becker, E. D.; Cabral De Menezes, S. M.; Goodfellow, R.; Granger, P. *Pure Appl. Chem.* **2001**, *73* (11), 1795. doi:10.1351/pac200173111795.
(45) Sheldrick, G. M. University of Gottingen, Germany, SHELXL-97, 1997.
(46) Beurskens, P. T.; Admiraal, G.; Beurskens, G.; Bosman, W. P.; de Gelder, R.; Israel, R.; Smits, J. M. M. Technical Report of the Crystallography Laboratory: University of Nijmegen, 1999.
(47) Carruthers, J. R.; Watkin, D. J. *Acta Crystallogr. A* **1979**, *35* (4), 698. doi:10.1107/S0567739479001613.
(48) Cromer, D. T.; Waber, J. T. The Kynoch Pres: Birmingham, 1974; Vol. IV.
(49) Ibers, J. A.; Hamilton, W. C. *Acta Crystallogr.* **1964**, *17* (6), 781. doi:10.1107/S0365110X64002067.
(50) Creagh, D. C.; McAuley, W. J.; Wilson, A. J. C., Ed. Kluwer Academic Publishers: Boston, 1992; Vol. C, pp 219–222.
(51) Creagh, D. C.; Hubbell, J. H.; Wilson, A. J. C., Ed. Kluwer Academic Publishers: Boston, 1992; Vol. C, pp 200–206.
(52) CrystalStructure; Rigaku and Rigaku Americas: 9009, New Trails Dr. The Woodlands, TX 77381, US, 2000–2007.
(53) Carruthers, J. R.; Rollett, J. S.; Betteridge, P. W.; Kinna, D.; Pearce, L.; Larsen, A.; Gabe, E. Chemical Crystallography Laboratory: Oxford, 1999.